energies

MDPI

Article

Research on Harmonic Current Amplification Effect of Parallel APF Compensating Voltage Source Nonlinear Load

Xueliang Wei [1], Cunzhong Li [2], Mingxuan Qi [2], Bingyang Luo [2], Xiangtian Deng [2] and Guorong Zhu [2,*]

[1] College of Geophysics and Information Engineering, China University of Petroleum-Beijing, Beijing 102249, China
[2] School of Automation, Wuhan University of Technology, Wuhan 430081, China
* Correspondence: zhgr_55@whut.edu.cn; Tel.: +86-189-7140-0950

Received: 10 June 2019; Accepted: 26 July 2019; Published: 9 August 2019

Abstract: A parallel active power filter (APF) is generally used to suppress dynamic harmonic current and compensate reactive power in the grid. However, parallel APF may have a negative effect on the load current when compensating the nonlinear load of a voltage source type, which may lead to the amplification effect of the load harmonic current. In this paper, the fundamental causes of harmonic current amplification were analyzed by studying the harmonic current amplification effect when a parallel APF compensates a nonlinear load. According to the results of the theoretical derivation, a feasible method to limit this current amplification effect by changing the system structure and the APF's own control was proposed, and the corresponding design scheme is given. Finally, the correctness of the theoretical derivation of the harmonic current amplification effect and the feasibility of the proposed solution were proven through simulation and experiment.

Keywords: parallel active power filter (APF); harmonic current amplification effect; compensation

1. Introduction

Diode uncontrolled rectifier converters have been widely used in switching power supply, AC servo drive (ASD), uninterruptible power supply (UPS), and other equipment due to the advantages of simple control and low cost. However, this type of converter injects a large amount of harmonic current into the power grid and is increasingly becoming the most important harmonic source in the power grid. According to whether the DC side of the uncontrolled rectifier bridge is connected with inductive or capacitive elements, it can be classified into a nonlinear load current source type and nonlinear load voltage source type.

In recent years, various studies have classified harmonic sources and filtering methods in detail, and studied the compensation characteristics of APF for different types of harmonic sources. Studies [1–5] have looked at the compensation of different types of loads by parallel APF and series APF from different perspectives, pointing out that parallel APFs are suitable for compensating current source type nonlinear harmonic sources and series APFs are suitable for compensating voltage source type nonlinear harmonic sources. Some studies have proposed methods of compensating voltage source type nonlinear load with parallel APFs, but research has only focused on the description, analysis and simulation of the phenomena generated when APF compensates a voltage source type nonlinear load, and fails to provide quantitative analysis and experimental verification [2–7]. Previous work [5] has pointed out that the original system is at risk of resonance and load current peak overcurrent when a parallel APF compensates for a capacitive non-linear load by analyzing the working process

of an uncontrolled rectifier non-linear load. The studies in [6,7] describe the characteristics and phenomena of parallel APF compensation motor and capacitor harmonic sources and converter harmonic source compensation.

An uncontrolled rectifier connected with a capacitor resistance load is looked upon as a typical voltage source type nonlinear load. Based on the study of the load characteristics, this paper focused on the harmonic current amplification effect of parallel APFs compensating for a typical voltage source type nonlinear load. A feasible method to limit the current amplification effect is proposed, and a brief design scheme is given. This paper illustrates that the equivalent impedance of the system side, the equivalent impedance of the load AC side, and the impedance characteristics of the load itself are the fundamental causes of the harmonic current amplification effect, and also provides quantitative analysis. The use of parallel APFs in compensating a voltage source type nonlinear load is limited by the harmonic current amplification effect. Finally, the simulation and experimental results prove that the theory of harmonic amplification effect is correct and the proposed solution feasible.

2. Research on Input Impedance of Voltage Source Type Nonlinear Load

Figure 1 shows the system main circuit structure of a parallel APF compensation voltage source type nonlinear load, where L_L is the impedance of the AC side of load and L_S is the equivalent impedance of the system side. L_S mainly includes two parts, namely the leakage inductance of the power transformer and the equivalent impedance of the transmission line. The structure in the dashed box in Figure 1 shows the typical resistance–capacitance uncontrolled rectifier nonlinear load.

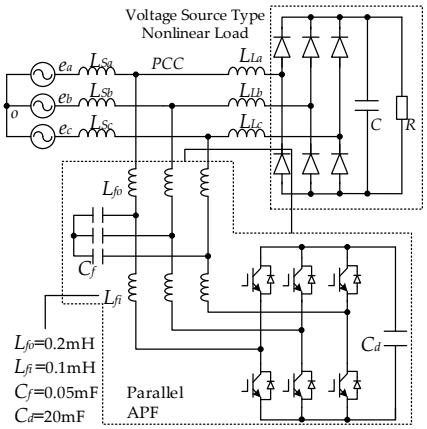

Figure 1. Parallel APF compensation voltage type nonlinear load main circuit.

If a capacitor filter is used behind the rectifier bridge and the capacitor is large enough, the DC side voltage of the rectifier bridge will remain basically constant and has similar characteristics to those of a voltage source, which can be equivalent to an ideal harmonic voltage source in series with an impedance. Additionally, the larger the capacitor value, the smaller the equivalent impedance; thus the closer the ideal harmonic voltage source in terms of characteristics. Therefore, as shown in Figure 2, the diode full-bridge rectifier circuit with capacitive filtering can be regarded as a voltage type harmonic source. The current research on APF compensation voltage-type harmonic sources is treated according to this approximate Thévenin equivalent [8–10].

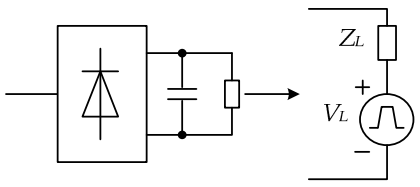

Figure 2. Equivalent harmonic voltage source.

Figure 3 shows an impedance diagram of the diode three-phase full bridge rectifier circuit. Assume that the current on the DC side is a continuous current, and the load connected behind the DC side is replaced by a resistor. In analyzing the circuit impedance with a small signal response, an important difference between the three-phase full-bridge rectifier circuit and the single-phase rectifier circuit is that the response of the three-phase rectifier circuit has an important relationship with its phase sequence [11,12]. This paper only focused on the positive order small signal response as an example, and gives the general steps of impedance analysis.

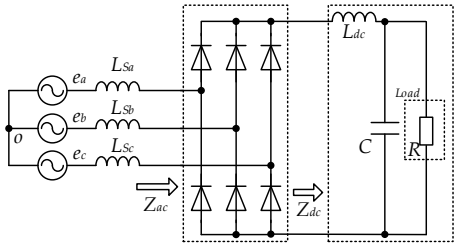

Figure 3. Impedance diagram of a three-phase full-bridge rectifier circuit.

Assume that the three-phase balanced positive sequence voltage is:

$$\begin{cases} v_a(t) = V_1 \sin(\omega_1 t) + V_p \sin(\omega_p t + \theta_p) \\ v_b(t) = V_1 \sin(\omega_1 t - \frac{2}{3}\pi) + V_p \sin(\omega_p t - \frac{2}{3}\pi + \theta_p) \\ v_c(t) = V_1 \sin(\omega_1 t + \frac{2}{3}\pi) + V_p \sin(\omega_p t + \frac{2}{3}\pi + \theta_p) \end{cases} \tag{1}$$

where V_P is the amplitude of the introduced small signal disturbance; ω_p and θ_p are the angular frequency and initial phase of the introduced small signal disturbance, respectively; and V_1 and ω_1 are the amplitude and angular frequency of the fundamental voltage of the system, respectively, where $V_1 > V_P$. According to the amplitude of the three-phase voltage, a mapping function is established. $\mathrm{Sgn}_i = 1$ ($i = a$, b or c) is defined when one phase voltage i is higher than the other two phases, $\mathrm{sgn}_i = -1$ is defined when the one phase voltage is lower than the other two phases, and $\mathrm{sgn}_i = 0$ is defined in the other cases. According to the defined switching function, the DC side voltage behind the rectifier bridge at this time can be expressed as a function of the three-phase voltage before the rectifier bridge, and the AC side current can be expressed as a function of the DC side current:

$$v_{dc}(t) = s_a(t)v_a(t) + s_b(t)v_b(t) + s_c(t)v_c(t) \tag{2}$$

$$\begin{cases} i_a(t) = s_a(t)i_{dc}(t) \\ i_b(t) = s_b(t)i_{dc}(t) \\ i_c(t) = s_c(t)i_{dc}(t) \end{cases} \tag{3}$$

The equation for the three-phase positive sequence mapping function in the frequency domain derived from [13–15] is as follows:

$$S_a[i] = \begin{cases} -\frac{(-1)^k j\sqrt{3}}{\pi(6k\pm1)} & i = (6k \pm 1)f_1 \\ \alpha \cos(\frac{2k\pi}{3} \mp \frac{\pi}{6}) e^{\mp j\frac{\pi}{2}} e^{jk\pi} & i = 2kf_1 \pm f_p \end{cases} \tag{4}$$

$$S_b[i] = \begin{cases} -\frac{(-1)^k j\sqrt{3} e^{\mp(j\frac{2}{3}\pi)}}{\pi(6k\pm1)} & i = (6k \pm 1)f_1 \\ \alpha \cos(\frac{2k\pi}{3} \mp \frac{\pi}{6}) e^{\mp j\frac{5\pi}{6}} e^{-\frac{jk\pi}{3}} & i = 2kf_1 \pm f_p \end{cases} \tag{5}$$

$$S_c[i] = \begin{cases} -\frac{(-1)^k j\sqrt{3} e^{\pm(j\frac{2}{3}\pi)}}{\pi(6k\pm1)} & i = (6k \pm 1)f_1 \\ \alpha \cos(\frac{2k\pi}{3} \mp \frac{\pi}{6}) e^{\mp j\frac{\pi}{6}} e^{\frac{jk\pi}{3}} & i = 2kf_1 \pm f_p \end{cases} \tag{6}$$

where $\alpha = Vpe \pm j\theta/\pi V_1$, and it can be seen from the above frequency domain equation that each phase's mapping function contains harmonics of $(6k \pm 1)f_1$, but harmonics are independent of disturbances. When the mapping function in the frequency domain form is determined, the input impedance in the case where the diode does not control the three-phase positive sequence of the rectifier bridge can be obtained through the following steps:

(1) According to Equation (2), the frequency domain convolution is performed between the three-phase AC input voltage and the obtained mapping function to calculate the frequency spectrum of the DC side voltage V_{DC}.
(2) According to the frequency spectrum of the obtained DC side voltage and the known DC side impedance, the frequency spectrum of the DC side current is calculated.
(3) According to Equation (3), the frequency domain convolution is performed between the obtained frequency spectrum of the DC side current and the switching function to calculate the frequency spectrum of the AC side current I_{AC}.

Based on Equations (2)–(6), the simplified input impedance of the three-phase rectifier bridge can be obtained as follows:

$$Z_{ac}(S) \approx \frac{\pi^2}{9}\left(\frac{1}{Z_{dc}(0)} + \frac{1}{Z_{dc}(s - j2\pi f_1)}\right)^{-1} \quad (7)$$

According to the obtained Equation (7), the impedance spectrum of the three-phase rectifier bridge with resistance and capacitance load was plotted. The main circuit parameters were the equivalent impedance of the system side: Ls = 90 μH, R_S = 0.5 Ω; resistance-capacitance load: C = 1 mF, R = 5 Ω; pure resistance load used to compare: R = 15 Ω, resistance–inductance load: R = 15 Ω, L = 2 mH, and its spectrum characteristics are shown in Figure 4.

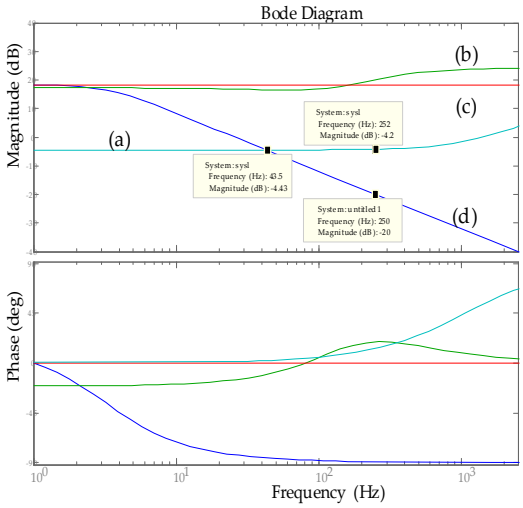

(a) The equivalent impedance of system side
(b) The input impedance of the resistance-inductance
(c)The input impedance of the pure resistance
(d)The input impedance of the resistance-capacitance load

Figure 4. Spectrum diagram of input impedance.

According to Figure 4, with the increase of frequency, the input impedance of the resistance–capacitance load's uncontrolled rectifier decreased rapidly, while the input impedance of the resistance–inductance and pure resistance uncontrolled rectifier changed very little and showed an upward trend. At this time, the input impedance of the resistance–capacitance load was −20 dB, the equivalent impedance of the system side was −4.2 dB, and the AC input impedance of the resistance–capacitance load was much smaller than the equivalent impedance of the system side. Moreover, with the increase in frequency, the equivalent impedance of the system side was larger and the AC input impedance was smaller. However, the pure resistance and resistance–inductance uncontrolled rectifier were opposite.

3. Analysis and Suppression Measures of Harmonic Current Amplification Effect

A parallel APF detects the harmonic current that need to be compensated, and then generates a compensation current of equal amplitude but opposite phase, and the current is injected into the common coupling point (PCC), so that the grid side can obtain the desired current and improve the power quality of the power grid. The parallel APF is connected to the PCC through an LCL filter, which is mainly used to filter out the switching ripple. The main parameters used in the experiment are shown in Figure 1.

3.1. Theoretical Derivation

Figure 5 is a single-phase fundamental equivalent circuit and a single harmonic equivalent circuit diagram of a parallel compensation system under an ideal power supply voltage, where λ is the harmonic current compensation rate, the voltage source V_{Lo} is a nonlinear load, Z_{Lo} is the input impedance of the nonlinear load, and the current source I_C is a parallel APF.

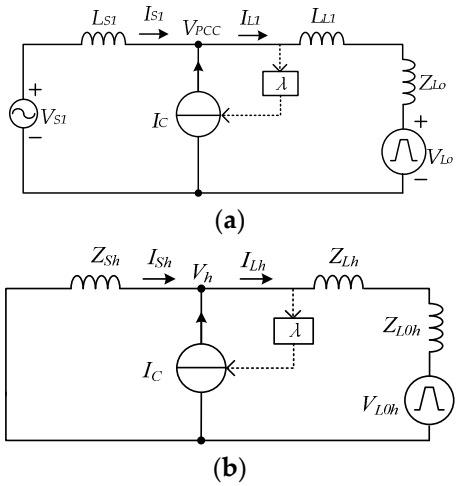

Figure 5. Single-phase equivalent circuit of parallel compensation voltage source type nonlinear load. (**a**) Single-phase fundamental equivalent circuit. (**b**) Single-phase harmonic equivalent circuit.

For the convenience of analysis, when only equivalent circuits at harmonic frequencies are studied, it is assumed that the power supply voltage does not contain harmonic components, the power grid is equivalent to a short circuit for harmonic frequencies, and the load is replaced by a single harmonic voltage source V_{Loh}, so a single-phase equivalent circuit is as shown in Figure 5b. The analysis can be divided into the following situations:

3.1.1. Parallel APF Fully Compensates Harmonic Current under Ideal Power Supply Voltage

Before parallel APF compensation, the current source I_C branch is equivalent to an open circuit, the APF compensation current $I_C = 0$, the system current I_{sh} is equal to the load current I_{Lh}, and the harmonic voltage at the PCC point is shown in Equation (8).

$$V_h = -I_{sh}Z_{sh} = (Z_{Lh} + Z_{Loh})I_{Lh} + V_{Loh} \tag{8}$$

Assuming that the APF completely compensates for the load harmonic current, when the system reaches a new balance after the APF compensates, $I'_{Sh} = 0$, and the compensation current I_C of the APF is equal to the load harmonic current, $I'_{Lh} = I_C$. At this time, the load AC side harmonic voltage V_{Loh} also changes, μ is defined as the AC side voltage change coefficient before and after compensation, and for a single harmonic voltage, the PCC point voltage after compensation is:

$$V_h = -I_{sh}'Z_{sh} = (Z_{Lh} + Z_{Loh})I_{Lh}' + V_{Loh}' = 0 \tag{9}$$

Simultaneously, Equations (8) and (9) can be derived:

$$\begin{cases} I_{Lh}(Z_{Sh} + Z_{Lh} + Z_{Loh}) + V_{Loh} = 0 \\ I_{Lh}'(Z_{Lh} + Z_{Loh}) + \mu V_{Lh} = 0 \end{cases} \tag{10}$$

According to the above equation, the harmonic current of the load before and after parallel APF compensation has the following relationship for the voltage source type nonlinear load under study.

$$\frac{I_{Lh}'}{I_{Lh}} = \mu \frac{Z_{Sh} + Z_{Lh} + Z_{Loh}}{Z_{Loh} + Z_{Lh}} = \mu(1 + \frac{Z_{Sh}}{Z_{Lh} + Z_{Loh}}) \tag{11}$$

3.1.2. Parallel APF Partially Compensates Harmonic Current under Ideal Power Supply Voltage

In practical application, an APF cannot fully compensate the load harmonic current due to the existence of a delay in the digital control and the limitation of the controller bandwidth. Assuming a harmonic current compensation rate of λ, APF will compensate the current $I_C = \lambda I_{Lh}'(0 < \lambda < 1)$, system harmonic current $I_{Sh}' = (1 - \lambda)I_{Lh}'$, and load AC side voltage $V_{Loh}' = \mu V_{Loh}$ after it is put into operation. At this point, the PCC point voltage after compensation is:

$$V_h = -I_{sh}'Z_{sh} = (Z_{Lh} + Z_{Loh})I_{Lh}' + V_{Loh}' \tag{12}$$

Simultaneously, Equations (8) and (12) can be derived:

$$\begin{cases} I_{Lh}(Z_{Sh} + Z_{Lh} + Z_{Loh}) + V_{Loh} = 0 \\ (1 - \lambda)I_{Lh}'Z_{Sh} + I_{Lh}'(Z_{Lh} + Z_{Loh}) + \mu V_{Loh} = 0 \end{cases} \tag{13}$$

According to Equation (13), the harmonic current of the load before and after parallel APF compensation has the following relationship:

$$\begin{aligned} \frac{I_{Lh}'}{I_{Lh}} &= \mu \frac{Z_{Sh} + Z_{Lh} + Z_{Loh}}{(1-\lambda)Z_{Sh} + Z_{Loh} + Z_{Lh}} \\ &= \mu(1 + \frac{\lambda}{(1-\lambda) + (Z_{Lh} + Z_{Loh})/Z_{Sh}}) \end{aligned} \tag{14}$$

Comparing Equation (14) with Equation (11), it can be seen that Equation (14) can be written as Equation (11) when λ = 1, that is, Equation (11) is a special case of Equation (14), so Equation (14) can be used as a general expression to describe the harmonic current amplification effect.

Assuming that the system power supply voltage is distorted, the single-phase harmonic equivalent circuit can be simplified as shown in Figure 6. According to the above similar analysis, it can be obtained that in the case of complete compensation, there is a relationship as shown in Equation (15) before and after compensation:

$$\begin{cases} I_{Lh}(Z_{Sh} + Z_{Lh} + Z_{Loh}) + V_{Loh} = V_{Sh} \\ I_{Lh}'(Z_{Lh} + Z_{Loh}) + \mu V_{Loh} = V_{Sh} \end{cases} \tag{15}$$

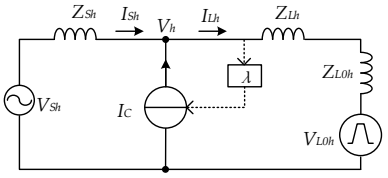

Figure 6. Single-phase equivalent circuit of parallel APF compensation voltage source type nonlinear load under a distorted system voltage.

At this time, it can be deduced that in the case of a distorted power supply, after a parallel APF completely compensates for a single harmonic, the change of a single harmonic before and after

compensation is exactly the same as Equation (11), that is, the distortion of the system voltage has no effect on the change of the load current before and after compensation. Similarly, it can be deduced that the change formula of a single harmonic before and after compensation is the same as Equation (14) under the case of partial compensation of the load current. Therefore, this paper used Equation (14) as a general formula to analyze the harmonic amplification effect.

3.2. Analysis of Harmonic Amplification Effect

The AC side voltage variation coefficient of the voltage source type nonlinear load is determined by the switching characteristics of the nonlinear load itself and the DC side voltage, and has little relationship with the AC side. Therefore, μ is temporarily taken to be equal to 1 in order to simplify the analysis, as can be seen from Figure 4, and the influence of the input impedance of the rectifier bridge on the harmonic current amplification effect can be ignored in the analysis. As a result, for the load studied in this paper, the harmonic current amplification effect was only related to the load harmonic current compensation rate, the system equivalent impedance, and the equivalent impedance of AC side of load. Therefore, for the loads used herein, Equation (14) can be simplified to:

$$\frac{I_{Lh}'}{I_{Lh}} = 1 + \frac{\lambda}{(1-\lambda) + Z_{Lh}/Z_{Sh}} \tag{16}$$

The equivalent impedances of the system side are the leakage inductance of the power transformer and the equivalent impedance of the transmission line, which can generally be considered unchanged. If the load is only connected to the PCC point through a section of ordinary wire, its impedance of the AC side is only the equivalent impedance of this wire, that is, Z_{Lh} is very small, even far less than the equivalent impedance of the system side. The harmonic compensation rate should generally reach more than 90%. Therefore, take $0.8 < \lambda < 1$, $0 < Z_{Lh}/Z_{Sh} < 1$. Assuming $Z_{Lh}/Z_{Sh} = 0.01$, if the APF harmonic is completely compensated, the load harmonic current will be amplified to 100 times before compensation.

The three-dimensional relationship of the harmonic amplification factor, harmonic compensation ratio, and impedance ratio is shown in Figure 7. As can be seen from Figure 7, when the ratio of the AC impedance of the load to the equivalent impedance of the system side is constant, the amplification factor of the harmonic current increases with an increase in the harmonic compensation accuracy. When the harmonic compensation rate is constant, with the decrease in the impedance ratio, the amplification factor of the harmonic current after compensation is larger. When the impedance ratio is close to 0 and the compensation accuracy is close to 100%, the harmonic amplification is close to infinity.

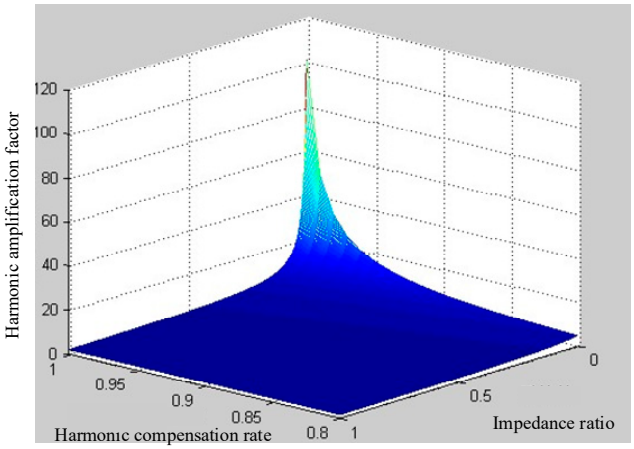

Figure 7. Three-dimensional relationship diagram of the harmonic magnification, harmonic compensation rate, and impedance ratio.

The load harmonic amplification effect is the result of the parallel APF itself, the nonlinear load, and the system. In the process of parallel APF outputting the compensation current, the load harmonic current increases continuously while the APF outputs a larger compensation current according to the detected load side harmonic current. This is equivalent to a kind of "positive feedback". When the system reaches a new balance without considering the APF capacity limit, the system will regain stability.

However, the harmonic current amplification effect will cause serious harm. First, the increase in the harmonic current load will affect the normal operation of its own equipment, shorten the service life of the equipment, or cause electromagnetic interference and other problems. In serious cases, the load may even exceed its capacity limit, resulting in damage to the load. Due to load harmonic current amplification, it is easy to exceed the APF's compensation capability, resulting in saturation or overcurrent.

3.3. Measures to Suppress Harmonic Amplification Effect

From the above analysis, it can be seen that for the three-phase full bridge rectifier circuit studied in this paper, the amplification effect of the load harmonic current was mainly related to three parameters. The smaller the equivalent impedance value of the system side, the better. However, the equivalent impedance value of the system side is difficult to change in actual systems. The load harmonic compensation rate can be easily changed in the APF control program, and the impedance value of the AC side of the load can also be easily changed through a simple modification of the system. Therefore, in order to suppress the amplification effect of the load harmonic current, this paper was conducted from the two aspects of the system structure and APF's own control.

3.3.1. AC Side of Load Is Connected in Series with Inductor

It can be seen from Equation (16) that increasing the impedance on the AC side of the load can reduce the amplification factor of the load harmonic current when the equivalent impedance of the system side keeps constant. The larger the series inductance, the better the effect of suppressing the harmonic current amplification. However, if the impedance value of the AC side of the load connected in series is too large, the voltage drop across this impedance will be large, resulting in a voltage drop on the DC side of the rectifier. Additionally, the reactive power of the system is increased. If the series inductance is too small, the suppression effect is difficult to play.

As is widely known, compared with passive power filters, APFs have great difficulty in application due to the increased costs. Generally speaking, the larger the APF capacity, the higher the cost. In engineering practice, the APF's capacity is calculated according to the load harmonic current, and the APF capacity is proportional to the effective value of system harmonics. Therefore, the amplification effect of the load harmonic current is proportional to the increase in APF capacity. Define the APF's capacity increase as follows: $m = I_{Lh}{}'/I_{Lh}$. When an APF is used to compensate the voltage source load, the corresponding APF capacity will be increased by 120%, while the harmonic after compensation is amplified to 120% before compensation. In order to reduce the cost of harmonic control, the more economical way is to use harmonic control devices to control the harmonic content of the current on the system side just within the standard, and define the residual harmonic content as the ratio of the harmonic content on the system side after compensation to the harmonic content before compensation, i.e., $1 - \lambda$. The voltage source type three-phase full bridge rectifier load studied in this paper could basically meet the standard of harmonic compensation when the harmonic compensation rate was 90%. Therefore, starting from reducing the cost of APF in engineering applications, this paper provides a standardized method to determine the impedance value of the AC side.

First, according to the specific conditions of the load, the value of the harmonic compensation rate λ is determined if the standard is met. Second, the equivalent impedance of the system side is determined according to the specific working conditions. Then, the above-mentioned values are substituted into the simplified Equation (16), and the magnitude of the impedance value on the AC side

of the load to be connected in series is derived according to the value of m, as shown in Equation (17). Figure 8 shows the relationship between the corresponding series impedance value and the required capacity of the APF when the harmonic compensation rates were 85%, 90%, and 95%, respectively. It can be seen from the figure that when the APF capacity increased a little, a considerable reactance needs to be connected in series on the AC side of the load, but with an increase in the APF capacity, the series reactance value will not change much. In the specific engineering design, it is also necessary to consider the impact of the impedance value of the AC side of the serial load on the fundamental voltage drop and system power consumption.

$$Z_{Lh} = \frac{1 - m - m\lambda}{m - 1} Z_{sh} \tag{17}$$

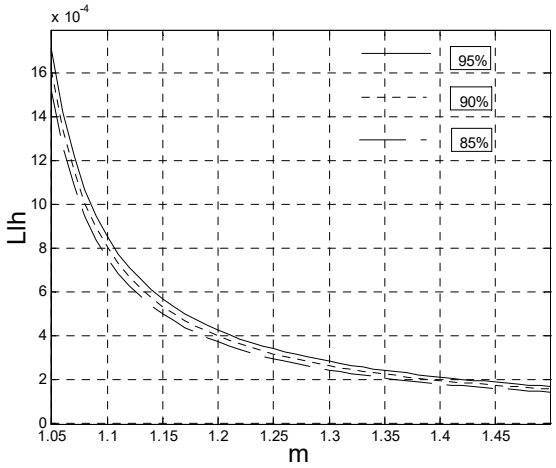

Figure 8. The magnitude of the required series impedance value.

3.3.2. Changing the Output Current of the Parallel APF

The amplification of harmonics can be reduced by appropriately reducing the compensation rate of parallel APF for some harmonic currents. Based on Equation (16), Assuming Z_{Lh}/Z_{Sh} = 0.01, the harmonic compensation rate will be reduced from 1 to 0.9 and the harmonic amplification will be reduced from 100 to 9.182. However, if the impedance on the AC side of the load is very small, the limitation of this method on the harmonic amplification effect is also limited.

4. Simulation, Experiment, and Result Analysis

4.1. Parallel APF Control Strategy

In this paper, the parallel APF adopted the control method based on load current detection, and Figure 9 is the control block diagram of the APF. The control of the APF is mainly completed by a digital signal processor (DSP), the detected signal is input to DSP after A/D conversion, the compensation current command generation, the current control and state space vector PWM modulation are completed in sequence, and the PWM pulses are sent out to control the on–off of the converter's main power device.

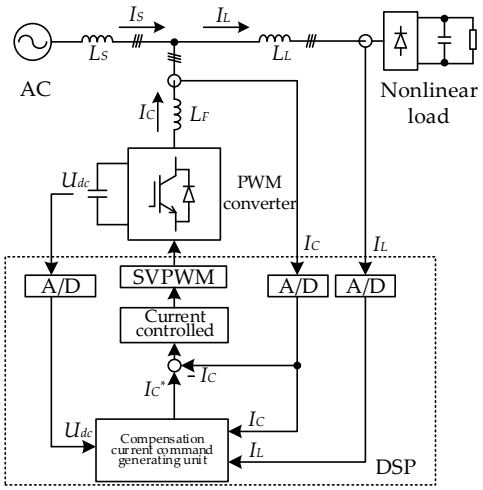

Figure 9. Control block diagram of parallel APF.

The key part of the APF control system is the compensation current command generation unit, which adopts the frequency division control scheme described above, and its block diagram is shown in Figure 10. The system-side equivalent impedance used in the simulation and experimental system is consistent with the theoretical analysis in the previous section, Ls = 90 μH, DC-side capacitance C = 7 mF, and resistance R = 15 Ω. The harmonic current I_{Lh} obtained by processing the load current I_L and filtering out the fundamental component is the main part of the compensation current command. However, due to the performance limitation of the filter, the extracted harmonic current cannot fully reflect the actual harmonic condition of the load current, so the specified subharmonic frequency division control method in the harmonic synchronous rotating coordinate system is adopted [16–20]. As shown in Figure 10, load current I_L minus the APF compensation current I_C equals the system current, the system current is transformed by n times of synchronous rotation coordinates to convert the n-th harmonic components into a direct current, which is extracted by a low-pass filter and then PI controlled. The traditional PI regulator can theoretically track the DC constant signal without static error and has good steady-state accuracy and dynamic response performance, so it can compensate the specified n-th harmonics efficiently.

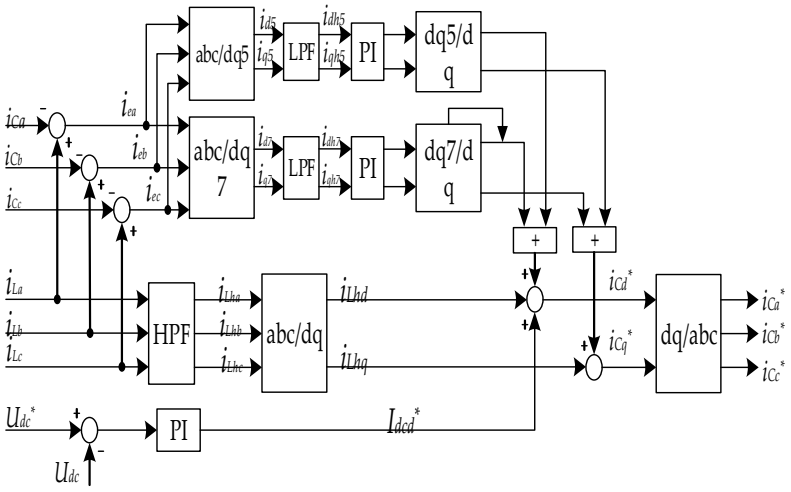

Figure 10. Compensation current command generation unit.

4.2. Simulation Results and Analysis

In order to verify the theoretical, a simulation model was built with MATLAB/Simulink for qualitative and quantitative analysis.

Figure 11 shows the dynamic waveform of the parallel APF compensation voltage source type nonlinear load when the series inductance L_L = 50 μH on the AC side of the load. The load current, system current, and APF compensation current were sequential from top to bottom. The parallel APF started to output compensation current at 0.15 s, the peak load current gradually increased from 82 A to 108 A, and the THD increased from 92.74 to 115.05%. Due to the small series inductance, the amplification effect of the load harmonic current after compensation was obvious and the compensation effect was not good, with the system current THD after compensation being 12.42%.

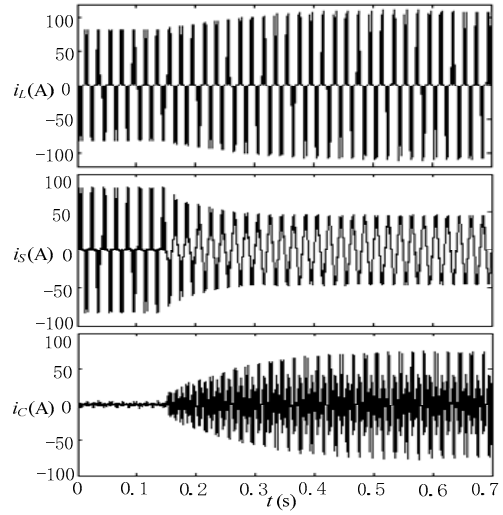

Figure 11. Dynamic waveform during APF compensation.

Figure 12 shows the waveform after the APF turned on the harmonic compensation to steady state when the series inductance L_L = 100 μH. Since the load THD reached 84.96% before compensation was added to the series inductor, the system current reached a better sine after compensation, and the THD was 4.96% after FFT analysis.

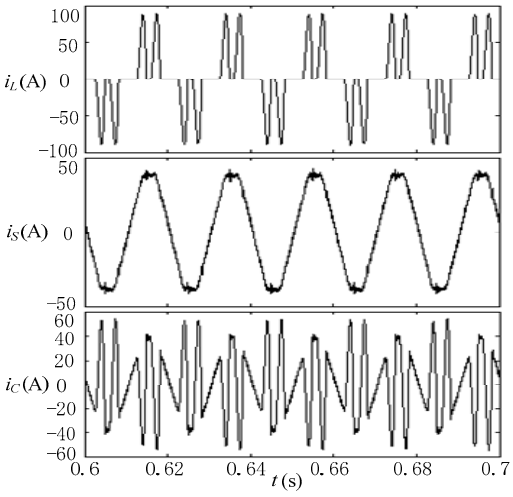

Figure 12. Steady-state waveform of the 100 μH inductor.

Figure 13 shows the waveform after the APF turns on harmonic compensation to steady state when series inductance L_L = 250 μH. Compared with the case of the 100 μH series connection, the sine of the system current waveform was further improved after compensation, and its THD was reduced to 3.61% after compensation.

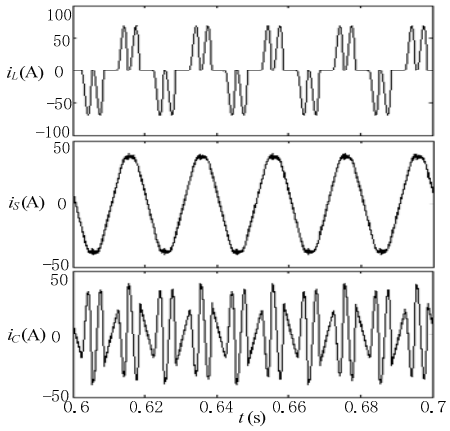

Figure 13. Steady state waveform of the 250 μH inductor.

Table 1 shows the FFT analysis results of the voltage and current waveforms before and after compensation for series inductance L_L = 100 μh, where V_{LO} is the load AC side voltage, and I_S and I_L are the system current and load current, respectively. This paper mainly analyzed the 5th, 7th, 11th, 13th, 17th, and 19th order characteristic harmonics with lower frequency. For the higher order harmonics, there will be larger errors due to control accuracy and delay, so they were not listed.

Table 1. Simulation results of series 100 μH inductors.

Parameters	Before Compensation		After Compensation		
	V_{Lo}	I_S, I_L	V_{Lo}'	I_S'	I_L'
THD	4.24%	85.46%	3.32%	4.96%	100.31%
Fun.	219 V	27.7 A	219.1 V	28.32 A	28.15 A
5th	2.62%	69.46%	1.6%	3.00%	76.77%
7th	2.47%	46.71%	1.7%	2.52%	58.09%
11th	1.00%	12.00%	1.02%	0.86%	22.45%
13th	0.80%	8.20%	0.62%	0.31%	11.65%
17th	0.79%	6.13%	0.56%	0.25%	7.90%
19th	0.57%	3.97%	0.54%	0.46%	6.68%

According to Table 1, the harmonic current amplification factor of each load can be calculated directly. Take 5 times as an example, the measured value of harmonic amplification factor is:

$$\eta = \frac{I_{L5}'}{I_{L5}} = \frac{28.15 \times 76.77\%}{27.7 \times 69.46\%} = 1.123 \tag{18}$$

The APF's compensation rate for the 5th harmonic current is:

$$\lambda = \frac{I_{L5}' - I_{S5}'}{I_{L5}'} = \frac{21.6 - 28.32 \times 3\%}{21.6} = 0.961 \tag{19}$$

The rate of change of the 5th harmonic component of the AC side voltage of the load is:

$$\mu = \frac{V_{Lo5}'}{V_{Lo5}} = \frac{219 \times 1.6\%}{219 \times 2.62\%} = 0.611 \tag{20}$$

The theoretical value of the amplification factor of the load's 5th harmonic current calculated according to Equation (16) is:

$$\eta^* = \frac{I_{L5}'}{I_{L5}} = 0.611 \times (1 + \frac{0.961}{1 - 0.961 + 10/9}) = 1.122 \tag{21}$$

Similarly, calculate the 7th, 11th, 13th, 17th, and 19th harmonic current amplification to obtain the calculation results shown in Table 2.

Table 2. Simulation results.

Parameters	Harmonic Compensation Rate λ	Voltage Change Rate μ	Harmonic Amplification Factor η		
			Measured Value	Theoretical Value	Error
5th	0.961	0.611	1.123	1.122	0.09%
7th	0.956	0.689	1.264	1.259	0.40%
11th	0.961	1.020	1.901	1.872	1.53%
13th	0.973	0.775	1.444	1.438	0.42%
17th	0.968	0.709	1.310	1.309	0.08%
19th	0.931	0.948	1.710	1.696	0.82%

It can be seen from Table 2 that the theoretical value of the harmonic current amplification calculated by Equation (7) is in good agreement with the simulated measured value, which shows the correctness of the theoretical derivation. At the same time, it can be seen from Table 2 that for different harmonics, the harmonic amplification values were not the same for approximately the same load harmonic compensation rate, which means that if the single harmonic is used as the capacity calculation reference, then the AC impedance required for series calculation is also different. Therefore, it is recommended that a single harmonic with the highest harmonic content is selected as the reference for estimation in practical engineering applications.

4.3. Experimental Results and Analysis

The parallel APF was a three-phase three-wire 66 kVA prototype developed by the laboratory, the DSP used in the control system was TMS320F2812, and the IGBT module of model SEMIX302GB12E4S was used as the main power device.

Figure 14a shows the experimental waveform when the series inductor is 100 μH, and Figure 14b shows the experimental waveform when the series inductor is 250 μH. From top to bottom, there are load current, system current and APF compensation current. As can be seen from Figure 14, the peak value of the load current and the peak value of APF output compensation current are smaller when the 250 μH inductor is connected in series than when the 100 μH inductor is connected in series, indicating that the larger the series inductor is, the better the suppression of load harmonics is.

The harmonic components of each voltage and current were measured by a Fluke Power Quality Analyzer, and the results shown in Table 3 were obtained.

Table 3. Experimental Results.

(a) Series Inductance 100 μH.					
Parameters	Before Compensation		After Compensation		
	V_L	I_S, I_L	V_L	I_S	I_L
Fun.	224.2 V	27.5 A	225.1 V	28.4 A	27.4 A
THD	3.9%	78%	3.0%	8.5%	93.1%
5th	2.7%	64.9%	1.6%	1.1%	72.6%
7th	2.2%	40.2%	1.5%	1.3%	52.0%
(b) Series Inductance 250 μH.					
Parameters	Before Compensation		After Compensation		
	V_L	I_S, I_L	V_L	I_S	I_L
Fun.	224 V	26.6 A	223.7 V	27.8 A	26.3 A
THD	5%	64.6%	4.6%	7.1%	76.2%
5th	3.6%	55.2%	3.0%	1.1%	63.5%
7th	2.7%	29.3%	2.5%	1.3%	38.0%

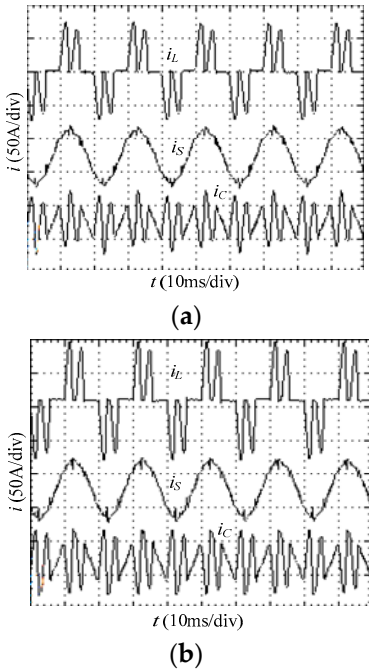

Figure 14. Experimental waveforms. (**a**) Series inductance 100 μH. (**b**) Series inductance 250 μH.

It can be seen from the table that regardless of whether the series inductance was 100 μH or 250 μH, the 5th and 7th harmonic components of the system current I_S after APF compensation were reduced to 1.1% and 1.3%, respectively, and good harmonic suppression effect was achieved. Since only the 5th and 7th harmonic currents were controlled by the composite control, the total harmonic distortion rate (THD) of the compensated system current was only reduced to 8.5% and 7.1%, respectively, and the effect was not ideal.

Table 4 also reflects the suppression effect of series inductance on the harmonic content and harmonic amplification effect. The load current THD before compensation was 78% when connected in series with a 100 μH inductor and 64.6% when connected in series with a 250 μH inductor. After compensation, the load current THD was 93.1% when 100 μH inductors were connected in series and 76.2% when 250 μH inductors were connected in series. The same effect was obtained for each harmonic component.

Table 4. Experimental calculation results.

Series Inductance	Harmonic Number	Harmonic Amplification Factor η		
		Measured Value	Theoretical Value	Error
100 μH	5th	1.115	1.114	0.089%
	7th	1.289	1.272	1.32%
250 μH	5th	1.137	1.124	1.14%
	7th	1.282	1.242	3.12%

Generally speaking, the larger inductor in series was better than the smaller inductor in suppressing the load harmonic current, which can effectively reduce the output current of APF, but the larger inductor has disadvantages in terms of cost and volume, and the fundamental voltage drop and loss are also issues that need to be considered. Therefore, the selection of series inductance needs to be comprehensively considered according to the actual requirements such as performance and cost.

Table 4 shows the calculation results based on the experimental data, and gives the load harmonic current amplification factor when the series inductance is 100 μH and 250 μH, respectively. By comparing the measured value with the theoretical calculation value, it can be seen that the error

between the two was quite small, indicating that the theoretical derivation was consistent with the actual situation.

5. Conclusions

In order to make full use of the advantages of parallel APF and expand its application field, this paper studied the theory and application of parallel APF compensation for voltage source nonlinear loads based on the frequency division control strategy proposed above. The theoretical analysis showed that parallel APF will affect the load current when compensating for the voltage source type nonlinear load, resulting in the load harmonic current amplification effect. The harmonic current amplification factor of the load is mainly related to the system side impedance, the equivalent impedance of the load AC side, and the relative magnitude of the input impedance of the load itself. At the same time, the harmonic compensation rate of APF will also affect the harmonic current amplification factor. Based on the above analysis, a method of series inductance on the AC side of the load and changing the magnitude of the harmonic compensation rate was proposed to suppress the harmonic amplification effect. Through the above method, the parallel APF can effectively compensate the harmonic current of the voltage source type nonlinear load.

Author Contributions: Conceptualization and Formal analysis, X.W.; Investigation, C.L.; Resources, M.Q.; Supervision, X.D.; Validation, B.L.; Writing—original draft, X.W.; Writing—review & editing, G.Z.

Funding: This research was funded by National Natural Science Foundation of China grand number 51777146 and the Science and Technology Foundation of Guizhou province in China (No. LH-[2014]7369).

Conflicts of Interest: The authors declare no conflict of interest.

References

1. Peng, F.Z. Harmonic sources and filtering approaches. *IEEE Ind. Appl. Mag.* **2001**, *7*, 18–25. [CrossRef]
2. Lascu, C.; Asiminoaei, L.; Boldea, I.; Blaabjerg, F. Frequency Response Analysis of Current Controllers for Selective Harmonic Compensation in Active Power Filters. *IEEE Trans. Ind. Electron.* **2009**, *56*, 337–347. [CrossRef]
3. Biricik, S.; Ozerdem, O.C.; Redif, S.; Dincer, M.S. New hybrid active power filter for harmonic current suppression and reactive power compensation. *Int. J. Electron.* **2016**, *103*, 1397–1414. [CrossRef]
4. Wang, Q.; Yao, W.; Liu, J.; Wang, Z. Voltage type harmonic source and series active power filter adopting new control approach. In Proceedings of the Conference of the IEEE Industrial Electronics Society, San Jose, CA, USA, 29 November–3 December 1999.
5. Priyashree, S.; Pooja, A.B.; Mahesh, E.; Vidya, H.A. Harmonic suppression in a non-linear load using three phase shunt active power filter. In Proceedings of the 2016 Biennial International Conference on Power and Energy Systems: Towards Sustainable Energy (PESTSE), Bangalore, India, 21–23 January 2016; pp. 1–6.
6. Li, L.; Lee, K.; Bai, K.; Ouyang, X.; Yang, H. Inverse Models and Harmonics Compensation for Suppressing Torque Ripples of Multiphase Permanent Magnet Motor. *IEEE Trans. Ind. Electron.* **2018**, *65*, 8730–8739. [CrossRef]
7. Wang, L.; Han, X.; Ren, C.; Yang, Y.; Wang, P. A Modified One-Cycle-Control-Based Active Power Filter for Harmonic Compensation. *IEEE Trans. Ind. Electron.* **2018**, *65*, 738–748. [CrossRef]
8. Delbem, A.C.; Cury, J.A. Effect of application time of APF and NaF gels on microhardness and fluoride uptake of in vitro enamel caries. *Am. J. Dent.* **2002**, *15*, 169. [PubMed]
9. Rico, J.J.; Acha, E.; Miller, T.J.E. Harmonic domain modelling of three phase thyristor-controlled reactors by means of switching vectors and discrete convolutions. *IEEE Trans. Power Deliv.* **1996**, *11*, 1678–1684. [CrossRef]
10. Carpinelli, G.; Iacovone, F.; Russo, A.; Varilone, P.; Verde, P. Analytical modeling for harmonic analysis of line current of VSI-fed drives. *IEEE Trans. Power Deliv.* **1997**, *12*, 1736–1743. [CrossRef]
11. Sun, J.; Zhonghui, B.; Kamiar, J.K. Input impedance modeling of multipulse rectifiers by harmonic linearization. *IEEE Trans. Power Electron.* **2009**, *24*, 2812–2820.

12. Sun, J.; Karmiar, K.J. Small signal input impedance modeling and analysis of line commutated rectifiers. *IEEE Trans. Power Electron.* **2009**, *24*, 2338–2346.
13. Hu, L.; Yacamini, R. Calculation of harmonics and interharmonics in HVDC schemes with low DC side impedance. *IEE Proc. C Gener. (Transm. Distrib.)* **1993**, *140*, 469–476. [CrossRef]
14. Hu, L.; Yacamini, R. Calculation of harmonic interference in HVDC systems with unbalance. In Proceedings of the International Conference on AC and DC Power Transmission, London, UK, 17–20 September 1991.
15. Rashid, M.H.; Maswood, A.I. Analysis of three phase AC/DC convertors under unbaland supply conditions. *IEEE Trans.* **1988**, *24*, 449–455.
16. Tareen, W.U.; Mekhilef, S.; Seyedmahmoudian, M.; Horan, B. Active power filter (APF) for mitigation of power quality issues in grid integration of wind and photovoltaic energy conversion system. *Renew. Sustain. Energy Rev.* **2017**, *70*, 635–655. [CrossRef]
17. Lei, W.; Lam, C.S.; Wong, M.C. Modeling and Parameter Design of Thyristor-Controlled LC-Coupled Hybrid Active Power Filter (TCLC-HAPF) for Unbalanced Compensation. *IEEE Trans. Ind. Electron.* **2017**, *64*, 1827–1840.
18. Durna, E.; Yılmaz, I.; Ermiş, M. Suppression of Time-Varying Interharmonics Produced by Medium-Frequency Induction Melting Furnaces by a HAPF System. *IEEE Trans. Power Electron.* **2017**, *32*, 1030–1043. [CrossRef]
19. Huang, Z.; Wu, Q.; Ma, J.; Fan, S. An APF and MPC combined collaborative driving controller using vehicular communication technologies. *Chaos Solitons Fractals* **2016**, *89*, 232–242. [CrossRef]
20. Takx, R.A.; Krissak, R.; Fink, C.; Bachmann, V.; Henzler, T.; Meyer, M.; Nance, J.W.; Schoenberg, S.O.; Apfaltrer, P. Low-tube-voltage selection for triple-rule-out CTA: Relation to patient size. *Eur. Radiol.* **2017**, *27*, 2292–2297. [CrossRef] [PubMed]